

# Superfluidity of bosons on a deformable lattice

G. Jackeli<sup>†</sup> and J. Ranninger

*Centre de Recherches sur les Très Basses Températures, Laboratoire Associé à l'Université Joseph Fourier,  
Centre National de la Recherche Scientifique, BP 166, 38042, Grenoble Cédex 9, France*

(November 6, 2018)

We study the superfluid properties of a system of interacting bosons on a lattice which, moreover, are coupled to the vibrational modes of this lattice, treated here in terms of Einstein phonon model. The ground state corresponds to two correlated condensates: that of the bosons and that of the phonons. Two competing effects determine the common collective soundwave-like mode with sound velocity  $v$ , arising from gauge symmetry breaking: i) The sound velocity  $v_0$  (corresponding to a weakly interacting Bose system on a rigid lattice) in the lowest order approximation is reduced due to reduction of the repulsive boson-boson interaction, arising from the attractive part of phonon mediated interaction in the static limit. ii) the second order correction to the sound velocity is enhanced as compared to the one of bosons on a rigid lattice when the boson-phonon interaction is switched on due to the retarded nature of phonon mediated interaction. The overall effect is that the sound velocity is practically unaffected by the coupling with phonons, indicating the robustness of the superfluid state. The induction of a coherent state in the phonon system, driven by the condensation of the bosons could be of experimental significance, permitting spectroscopic detections of superfluid properties of the bosons. Our results are based on an extension of the Beliaev - Popov formalism for a weakly interacting Bose gas on a rigid lattice to that on a deformable lattice with which it interacts.

PACS numbers: 05.30.Jp, 67.57.Jj, 63.20.Mt, 67.90.+z

## I. INTRODUCTION

The weakly interacting Bose gas has been studied theoretically in great deal over the past fifty years; mainly in view of understanding the superfluid properties of  $^4\text{He}$  and its rich phase diagram in the temperature - pressure parameter space. These studies provided a qualitative description of the low temperature collective soundwave like spectrum, the depletion of the condensate, etc.<sup>1</sup> In more recent years attempts have been made to examine other systems than  $^4\text{He}$  which potentially could show such superfluid properties. The superfluidity of excitons in semiconducting materials such as  $\text{Cu}_2\text{O}$ , presents one of those novel systems.<sup>2</sup> There, the interaction between the excitons with acoustic phonons seems to play a key role in establishing such a superfluidity of the bosonic excitons. In fact it involves the appearance of a coherent crystal displacement field which enables a moving exciton-phonon condensate.<sup>3</sup>

In the present work we want to address ourselves to a general situation and consider the system in which the itinerant bosons, apart from an intrinsic repulsion between them, are coupled to some bosonic degrees of freedom, which for brevity we shall term *phonons*. For instance, this situation might be realized in short coherence length superconductors which are controlled by the fluctuations of the phase of the order parameter rather than of its amplitude. In such systems one expects relatively long lived local pairs of electrons which can be considered as hard-core Bosons on a lattice and which are coupled to the dynamical deformations of this underlying lattice.

Ion-channelling experiments<sup>4</sup> on High- $T_c$  cuprates (showing a drastic increase in the critical angle for Rutherford back-scattering just below  $T_c$ ), as well as optical absorption measurements<sup>5</sup> (showing a substantial increase in the phonon intensity just below  $T_c$ ) indicate that, upon entering the superconducting state, the uncorrelated motion of the local lattice vibrations might get correlated, resulting in the emergence of an acoustic branch in the phonon spectrum.

One also might think about systems, in which spin or pseudo-spin (orbital) degrees are coupled to the lattice. If, upon lowering the temperature, a long-range order due to the continuous symmetry breaking occurs in those systems, while the symmetry restoring variable is being coupled to the phonons, then the system will show the same physics associated with macroscopic quantum effects as the model we are going to deal with.

The study presented in the present paper is, to our knowledge, the first generalization of the known field-theoretical treatment of the weakly interacting dilute Bose gas when the effective two-body potential is supplemented by a time dependent retarded part stemming from the phonon mediated retarded interaction.

We shall study here the feasibility of such a phenomenon on the basis of a simple model of itinerant bosons on a deformable lattice. In the present work we consider lattices susceptible of local lattice deformations. Such local deformations occur in the systems built up of molecular units and manifest themselves as dynamical deformations which are à priori spatially uncorrelated and are described by the Einstein phonon model.

Generalization of such a scenario to globally deformable lattices, described by acoustic phonon modes, will be briefly mentioned in the concluding part of the paper and will be subject of a future publication. In section 2 we shall define the model and study it within the standard Bogoliubov scheme<sup>6</sup> which we extend to two interacting boson fields: that of the itinerant bosons (the local electron pairs or electron-hole pairs respectively) and that of representing the lattice degrees of freedom (the optical or acoustic phonons respectively). This approximation treats the scattering processes among condensate quasi-particles and between condensate and out-of-condensate quasi-particles, but neglects scattering among out-of-condensate quasi-particles. These latter processes are important if the system are not very dilute and if the temperature is finite. A consistent theory which can satisfactorily deal with that situation is the so called Beliaev-Popov theory<sup>7,8</sup>, which, in section 3, we shall generalize from a weakly interacting Bose gas on a rigid lattice to one where also the interaction between the bosons and the lattice vibrations are taken into account. In section 4 we address the question of the renormalization of the sound velocity of the collective modes in the hydrodynamic regime at temperature zero. We shall illustrate the subtle compensation between two competing mechanisms arising from the boson-phonon coupling which while leading to an enhancement of the boson mass it also leads to an increased rigidity of the phase of the condensate. As a result the sound velocity is practically the same as that for a weakly interacting Bose gas on a rigid lattice. Concluding remarks and an outlook on further studies are presented in section 5.

## II. THE MODEL AND ITS SOLUTION WITHIN A BOGOLIUBOV SCHEME

We consider a system of bosons on a lattice having a tight binding spectrum  $\epsilon_{\mathbf{q}} = zt[1 - 1/3(\cos q_x + \cos q_y + \cos q_z)]$  (From now on we shall set  $zt = 1$ , measuring all energies in units of the half bandwidth) which in the long wavelength limit is given by  $\epsilon_{\mathbf{q}} = q^2/2M$  with  $M$  being the the bare boson mass. The interaction between bosons is characterized by a coupling constant  $g$  and that between the bosons and the phonons by  $\alpha\omega_0$ ,  $\omega_0$  denoting the frequency of the optical phonon mode. The Hamiltonian for such a system is then given by

$$\begin{aligned}
H = & \sum_{\mathbf{q}} \epsilon_{\mathbf{q}} b_{\mathbf{q}}^{\dagger} b_{\mathbf{q}} + \omega_0 \sum_{\mathbf{q}} (a_{\mathbf{q}}^{\dagger} a_{\mathbf{q}} + \frac{1}{2}) \\
& + \frac{g}{2N} \sum_{\mathbf{k}, \mathbf{k}', \mathbf{p}} b_{\mathbf{k}}^{\dagger} b_{\mathbf{k}'}^{\dagger} b_{\mathbf{k}' - \mathbf{p}} b_{\mathbf{k} + \mathbf{p}} \\
& - \frac{\alpha\omega_0}{\sqrt{N}} \sum_{\mathbf{k}, \mathbf{q}} b_{\mathbf{k}}^{\dagger} b_{\mathbf{k} + \mathbf{q}} [a_{\mathbf{q}}^{\dagger} + a_{-\mathbf{q}}] \quad (1)
\end{aligned}$$

where  $b_{\mathbf{k}}^{(\dagger)}$  and  $a_{\mathbf{q}}^{(\dagger)}$  denote the boson and phonon annihilation (respectively creation) operators,  $\epsilon_{\mathbf{q}} = \epsilon_{\mathbf{q}} - \mu$  and

$\mu$  being the chemical potential. Let us now assume the existence of a condensed state not only for the bosons but also for the phonons and consequently make the Ansatz:

$$b_{\mathbf{k}} = \hat{b}_{\mathbf{k}} + \bar{b}\delta_{\mathbf{k},0}, \quad a_{\mathbf{k}} = \hat{a}_{\mathbf{k}} + \bar{a}\delta_{\mathbf{k},0} \quad (2)$$

By substituting expressions (2) into the Hamiltonian (1) and requiring that the terms linear in  $\hat{b}_{\mathbf{k}}$  and  $\hat{a}_{\mathbf{q}}$  vanish we find the following relations

$$\begin{aligned}
\bar{a} &= \frac{\alpha\bar{b}^2}{\sqrt{N}} = \alpha\sqrt{N}n_c \\
n_c &= \frac{\bar{b}^2}{N} \\
\mu &\rightarrow \bar{g}n_c, \quad \bar{g} = g - 2\alpha^2\omega_0. \quad (3)
\end{aligned}$$

finally yielding the following Hamiltonian

$$H = H_0 + H_{B-P} + H_{B-B} \quad (4)$$

and where

$$\begin{aligned}
H_0 &= \sum_{\mathbf{q}} \bar{\epsilon}_{\mathbf{q}} \hat{b}_{\mathbf{q}}^{\dagger} \hat{b}_{\mathbf{q}} + \omega_0 \sum_{\mathbf{q}} \hat{a}_{\mathbf{q}}^{\dagger} \hat{a}_{\mathbf{q}} \\
&+ \frac{gn_c}{2} \sum_{\mathbf{q}} [\hat{b}_{\mathbf{q}}^{\dagger} \hat{b}_{-\mathbf{q}}^{\dagger} + \hat{b}_{\mathbf{q}} \hat{b}_{-\mathbf{q}}] \\
&- \alpha\omega_0\sqrt{n_c} \sum_{\mathbf{q}} [\hat{b}_{\mathbf{q}}^{\dagger} + \hat{b}_{-\mathbf{q}}] [\hat{a}_{\mathbf{q}} + \hat{a}_{-\mathbf{q}}^{\dagger}] \quad (5)
\end{aligned}$$

with

$$\bar{\epsilon}_{\mathbf{q}} = \epsilon_{\mathbf{q}} + 2gn_c - 2\alpha^2\omega_0n_c = \epsilon_{\mathbf{q}} + gn_c. \quad (6)$$

The Hamiltonian  $H_0$  describes the Bogoliubov quasi-particles which are hybridized with the phonons. In the condensed state the single particle excitations hybridize with the density fluctuations due to the broken gauge symmetry and give rise to the collective excitation spectrum of the bosons with a sound-wave like spectrum. The phonons which initially couple to those density fluctuations hence get hybridized with those collective modes. The second term in the Hamiltonian Eq. (4) describes that coupling between the density of the out-of-condensate particles with the phonons.

$$H_{B-P} = -\frac{\alpha\omega_0}{\sqrt{N}} \sum_{\mathbf{k}, \mathbf{q}} \hat{b}_{\mathbf{k}}^{\dagger} \hat{b}_{\mathbf{k} + \mathbf{q}} [\hat{a}_{\mathbf{q}}^{\dagger} + \hat{a}_{-\mathbf{q}}]. \quad (7)$$

The last term in the Hamiltonian Eq. (4),  $H_{B-B}$ , describes the interaction between the out-of-condensate particles.

Let us next define a generalization of the standard Bogoliubov transformation

$$\begin{aligned}
\alpha_{\mathbf{q}} &= u_{1,\mathbf{q}}\hat{b}_{\mathbf{q}} + u_{2,\mathbf{q}}\hat{a}_{\mathbf{q}} + v_{1,\mathbf{q}}\hat{b}_{-\mathbf{q}}^{\dagger} + v_{2,\mathbf{q}}\hat{a}_{-\mathbf{q}}^{\dagger} \\
\beta_{\mathbf{q}} &= \bar{u}_{1,\mathbf{q}}\hat{b}_{\mathbf{q}} + \bar{u}_{2,\mathbf{q}}\hat{a}_{\mathbf{q}} + \bar{v}_{1,\mathbf{q}}\hat{b}_{-\mathbf{q}}^{\dagger} + \bar{v}_{2,\mathbf{q}}\hat{a}_{-\mathbf{q}}^{\dagger} \\
\alpha_{-\mathbf{q}}^{\dagger} &= u_{1,\mathbf{q}}\hat{b}_{-\mathbf{q}}^{\dagger} + u_{2,\mathbf{q}}\hat{a}_{-\mathbf{q}}^{\dagger} + v_{1,\mathbf{q}}\hat{b}_{\mathbf{q}} + v_{2,\mathbf{q}}\hat{a}_{\mathbf{q}} \\
\beta_{-\mathbf{q}}^{\dagger} &= \bar{u}_{1,\mathbf{q}}\hat{b}_{-\mathbf{q}}^{\dagger} + \bar{u}_{2,\mathbf{q}}\hat{a}_{-\mathbf{q}}^{\dagger} + \bar{v}_{1,\mathbf{q}}\hat{b}_{\mathbf{q}} + \bar{v}_{2,\mathbf{q}}\hat{a}_{\mathbf{q}}. \quad (8)
\end{aligned}$$

With the requirement that the new operators satisfy the standard canonical commutation relations for Bosons, we obtain the following relations between the coefficients of this transformation

$$\begin{aligned} [\alpha_{\mathbf{q}}, \alpha_{\mathbf{q}}^\dagger] &= 1 \Rightarrow u_{1,\mathbf{q}}^2 + u_{2,\mathbf{q}}^2 - v_{1,\mathbf{q}}^2 - v_{2,\mathbf{q}}^2 \\ [\beta_{\mathbf{q}}, \beta_{\mathbf{q}}^\dagger] &= 1 \Rightarrow \bar{u}_{1,\mathbf{q}}^2 + \bar{u}_{2,\mathbf{q}}^2 - \bar{v}_{1,\mathbf{q}}^2 - \bar{v}_{2,\mathbf{q}}^2 \end{aligned} \quad (9)$$

$$\begin{aligned} [\alpha_{\mathbf{q}}, \beta_{\mathbf{q}}^\dagger] &= 0 \Rightarrow u_{1,\mathbf{q}}\bar{u}_{1,\mathbf{q}} + u_{2,\mathbf{q}}\bar{u}_{2,\mathbf{q}} - v_{1,\mathbf{q}}\bar{v}_{1,\mathbf{q}} - v_{2,\mathbf{q}}\bar{v}_{2,\mathbf{q}} \\ [\alpha_{\mathbf{q}}, \beta_{-\mathbf{q}}] &= 0 \Rightarrow u_{1,\mathbf{q}}\bar{v}_{1,\mathbf{q}} + u_{2,\mathbf{q}}\bar{v}_{2,\mathbf{q}} - v_{1,\mathbf{q}}\bar{u}_{1,\mathbf{q}} - v_{2,\mathbf{q}}\bar{u}_{2,\mathbf{q}} \end{aligned}$$

The transformation, Eq. (8), diagonalizes the Hamiltonian  $H_0$ , bringing it into the form

$$\tilde{H}_0 = \sum_{\mathbf{q}} (\omega_{1,\mathbf{q}}\alpha_{\mathbf{q}}^\dagger\alpha_{\mathbf{q}} + \omega_{2,\mathbf{q}}\beta_{\mathbf{q}}^\dagger\beta_{\mathbf{q}}). \quad (10)$$

The eigen-frequencies  $\omega_{1,\mathbf{q}}$  and  $\omega_{2,\mathbf{q}}$  as well as the coherence factors are determined in the usual way by diagonalizing the secular equation for the variables  $\alpha_{\mathbf{q}}, \alpha_{-\mathbf{q}}^\dagger, \beta_{\mathbf{q}}, \beta_{-\mathbf{q}}^\dagger$  which leads to:

$$\begin{aligned} \omega_{1,2,\mathbf{q}}^2 &= \frac{E_{B\mathbf{q}}^2 + \omega_0^2}{2} \\ &\mp \frac{1}{2}\sqrt{[E_{B\mathbf{q}}^2 - \omega_0^2]^2 + 16\alpha^2\omega_0^3\varepsilon_{\mathbf{q}}n_c} \end{aligned} \quad (11)$$

$$\begin{pmatrix} u_1 \\ v_1 \end{pmatrix} = \frac{\omega_{1,\mathbf{q}} \pm \varepsilon_{\mathbf{q}}}{2\sqrt{\omega_{1,\mathbf{q}}\varepsilon_{\mathbf{q}}}} \sqrt{\frac{\omega_0^2 - \omega_{1,\mathbf{q}}^2}{\omega_{2,\mathbf{q}}^2 - \omega_{1,\mathbf{q}}^2}} \quad (12)$$

$$\begin{pmatrix} u_2 \\ v_2 \end{pmatrix} = \frac{\omega_{1,\mathbf{q}} \pm \omega_0}{2\sqrt{\omega_{1,\mathbf{q}}\omega_0}} \sqrt{\frac{E_{B\mathbf{q}}^2 - \omega_{1,\mathbf{q}}^2}{\omega_{2,\mathbf{q}}^2 - \omega_{1,\mathbf{q}}^2}} \quad (13)$$

$$\begin{pmatrix} \bar{u}_1 \\ \bar{v}_1 \end{pmatrix} = -\frac{\omega_{2,\mathbf{q}} \pm \varepsilon_{0,\mathbf{q}}}{2\sqrt{\omega_{2,\mathbf{q}}\varepsilon_{\mathbf{q}}}} \sqrt{\frac{\omega_{2,\mathbf{q}}^2 - \omega_0^2}{\omega_{2,\mathbf{q}}^2 - \omega_{1,\mathbf{q}}^2}} \quad (14)$$

$$\begin{pmatrix} \bar{u}_2 \\ \bar{v}_2 \end{pmatrix} = \frac{\omega_{2,\mathbf{q}} \pm \omega_0}{2\sqrt{\omega_{2,\mathbf{q}}\omega_0}} \sqrt{\frac{\omega_{2,\mathbf{q}}^2 - E_{B\mathbf{q}}^2}{\omega_{2,\mathbf{q}}^2 - \omega_{1,\mathbf{q}}^2}}, \quad (15)$$

and where  $E_{B\mathbf{q}} = \sqrt{\varepsilon_{\mathbf{q}}[\varepsilon_{\mathbf{q}} + 2gn_c]}$  denotes the spectrum of Bogoliubov quasi-particles in the absence of coupling with phonons.

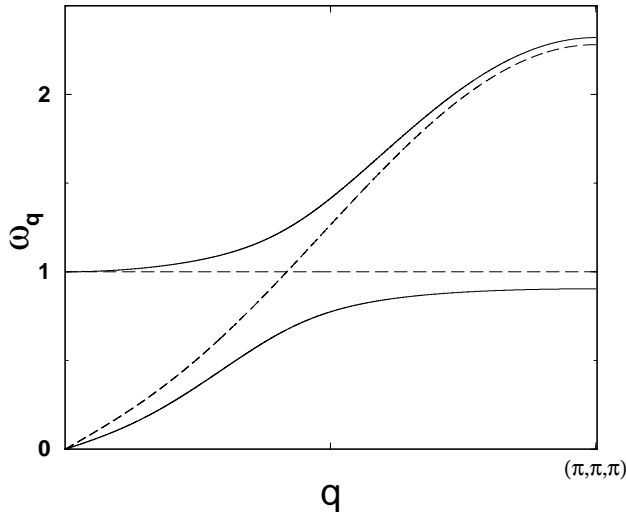


FIG. 1. Sketch of the excitation spectra  $\omega_{1,2,\mathbf{q}}$ , Eq. (11), in the lowest order approximation (solid line). The excitation spectra in the absence of boson-phonon coupling is represented by dashed lines.

In Fig. 1 we illustrate the two branches of eigen-frequencies  $\omega_{1(2),\mathbf{q}}$ . When  $E_{B\mathbf{q}}$  is not close to the phonon frequency  $\omega_0$ , then the two normal modes consist of a Bogoliubov excitation and a phonon mode; one of the modes being mainly a phonon and the other a Bogoliubov excitation. For  $E_{B\mathbf{q}}$  close to  $\omega_0$ , neither mode is predominantly a phonon or a bosonic excitation. The mode which is a phonon (Bogoliubov excitation) for  $E_{B\mathbf{q}} \ll \omega_0$  becomes a Bogoliubov excitation (phonon) for  $\omega_0 \ll E_{B\mathbf{q}}$ . In the long-wavelength limit the lower branch reduces to a sound-like dispersion

$$\omega_{1,\mathbf{q}} \simeq v_0 q, \quad \mathbf{q} \rightarrow 0, \quad (16)$$

with a characteristic sound velocity

$$v_0 = [(g - 2\alpha^2\omega_0)n_c/M]^{1/2}. \quad (17)$$

which is reduced in comparison to that where the boson-phonon coupling is absent. This reduction is determined by the static part of the attractive phonon mediated interaction.

The set of relations, Eqs. (11 - 15) represent the lowest order approximation to our problem, i.e., it takes into account collisions between condensate quasi-particles, between condensate and out-of-condensate quasi-particles, but totally neglects scattering among out-of-condensate quasi-particles as well as scattering out-of-condensate quasi-particles on phonons. As the concentration of quasi-particles increases these latter become important. We therefore shall have to include in our study the effect of  $H_{B-P}$  and  $H_{B-B}$ . In the next section, we shall generalize the Beliaev-Popov approximation (BPA)<sup>7,8</sup> for the case when the bosons, coupled together by the two-body potential, are moreover coupled by the phonon-mediated retarded interaction. Since in the BPA the second-order self-energies are built out of the mean-field propagators we shall define all the Green's functions involved in our perturbation theory and give their expression within the mean-field approximation. These propagators can be defined as the elements of a matrix Green's function composed of a four-component bosonic field  $\{b_{\mathbf{q}}, a_{\mathbf{q}}, b_{-\mathbf{q}}^\dagger, a_{-\mathbf{q}}^\dagger\}$ , the components of which are however related among each-other by symmetry relations. We define the canonical  $2 \times 2$  matrix Green's functions for bosons, with diagonal ( $\mathcal{G}$ ) and non-diagonal ( $\hat{\mathcal{G}}$ ) components; the phonon Green's functions ( $\mathcal{D}$ ) and the phonon-boson Green's function ( $\mathcal{H}$ ), that describes the hybridization of these two bosonic excitations in the condensed state

$$\begin{aligned}
\mathcal{G}_{\mathbf{q}}(\omega) &= \langle\langle b_{\mathbf{q}}|b_{\mathbf{q}}^{\dagger}\rangle\rangle_{\omega}, \quad \hat{\mathcal{G}}_{\mathbf{q}}(\omega) = \langle\langle b_{\mathbf{q}}|b_{-\mathbf{q}}\rangle\rangle_{\omega}, \\
\mathcal{D}_{\mathbf{q}}(\omega) &= \langle\langle a_{\mathbf{q}} + a_{-\mathbf{q}}^{\dagger}|a_{\mathbf{q}}^{\dagger} + a_{-\mathbf{q}}\rangle\rangle_{\omega}, \\
\mathcal{H}_{\mathbf{q}}(\omega) &= \langle\langle b_{\mathbf{q}}|a_{\mathbf{q}}^{\dagger} + a_{-\mathbf{q}}\rangle\rangle_{\omega}.
\end{aligned} \tag{18}$$

The mean-field Green's functions, introduced above, are obtained from the diagonalized Hamiltonian, Eq. (10), with the help of the inverse canonical transformation

$$\begin{aligned}
\hat{b}_{\mathbf{q}} &= u_{1,\mathbf{q}}\alpha_{\mathbf{q}} + \bar{u}_{1,\mathbf{q}}\beta_{\mathbf{q}} - v_{1,\mathbf{q}}\alpha_{-\mathbf{q}}^{\dagger} - \bar{v}_{1,\mathbf{q}}\beta_{-\mathbf{q}}^{\dagger} \\
\hat{a}_{\mathbf{q}} &= u_{2,\mathbf{q}}\alpha_{\mathbf{q}} + \bar{u}_{2,\mathbf{q}}\beta_{\mathbf{q}} - v_{2,\mathbf{q}}\alpha_{-\mathbf{q}}^{\dagger} - \bar{v}_{2,\mathbf{q}}\beta_{-\mathbf{q}}^{\dagger} \\
\hat{b}_{-\mathbf{q}}^{\dagger} &= -v_{1,\mathbf{q}}\alpha_{\mathbf{q}} - \bar{v}_{1,\mathbf{q}}\beta_{\mathbf{q}} + u_{1,\mathbf{q}}\alpha_{-\mathbf{q}}^{\dagger} + \bar{u}_{1,\mathbf{q}}\beta_{-\mathbf{q}}^{\dagger} \\
\hat{a}_{-\mathbf{q}}^{\dagger} &= -v_{2,\mathbf{q}}\alpha_{\mathbf{q}} - \bar{v}_{2,\mathbf{q}}\beta_{\mathbf{q}} + u_{2,\mathbf{q}}\alpha_{-\mathbf{q}}^{\dagger} + \bar{u}_{2,\mathbf{q}}\beta_{-\mathbf{q}}^{\dagger}.
\end{aligned} \tag{19}$$

This leads to the following expressions for those mean-field Green's functions

$$\begin{aligned}
\mathcal{G}_{\mathbf{q},\omega} &= \frac{u_{1,\mathbf{q}}^2}{\omega - \omega_{1,\mathbf{q}}} - \frac{v_{1,\mathbf{q}}^2}{\omega + \omega_{1,\mathbf{q}}} + [\omega_{1,\mathbf{q}}, u, v \rightarrow, \omega_{2,\mathbf{q}}, \bar{u}, \bar{v}], \\
\hat{\mathcal{G}}_{\mathbf{q},\omega} &= -u_{1,\mathbf{q}}v_{1,\mathbf{q}}\frac{2\omega_{1,\mathbf{q}}}{\omega^2 - \omega_{1,\mathbf{q}}^2} + [\omega_{1,\mathbf{q}}, u, v \rightarrow, \omega_{2,\mathbf{q}}, \bar{u}, \bar{v}], \\
\mathcal{D}_{\mathbf{q},\omega} &= (u_{2,\mathbf{q}} - v_{2,\mathbf{q}})^2\frac{2\omega_{1,\mathbf{q}}}{\omega^2 - \omega_{1,\mathbf{q}}^2} + [\omega_{1,\mathbf{q}}, u, v \rightarrow, \omega_{2,\mathbf{q}}, \bar{u}, \bar{v}], \\
\mathcal{H}_{\mathbf{q},\omega} &= (u_{2,\mathbf{q}} - v_{2,\mathbf{q}})\left[\frac{u_{1,\mathbf{q}}}{\omega - \omega_{1,\mathbf{q}}} + \frac{v_{1,\mathbf{q}}}{\omega + \omega_{1,\mathbf{q}}}\right] \\
&\quad + [\omega_{1,\mathbf{q}}, u, v \rightarrow, \omega_{2,\mathbf{q}}, \bar{u}, \bar{v}].
\end{aligned} \tag{20}$$

In Fig. 2 we express graphically the phonon  $\mathcal{D}$  and the boson-phonon  $\mathcal{H}$  Green's functions in terms of  $\mathcal{G}$ , the normal and  $\hat{\mathcal{G}}$ , the anomalous component of the boson Green's functions. The choice of this graphical representation is convenient when constructing all the second-order self-energy diagrams, as will be discussed in the next section. The full straight lines with two arrows in the same (opposite) direction represent the normal (anomalous) component of boson Green's function. The thin wavy and bold wavy lines stand for the bare and the mean field Green's functions of the phonons. The boson-phonon Green's functions are built up of a wavy line and an outgoing straight line. The dot represents the boson-phonon vertex and the zig-zag line the condensate (given by a factor  $n_c^{1/2}$ ).

FIG. 2. Graphical representation for the mean field Green's functions  $\mathcal{D}$  and  $\mathcal{H}$ .

### III. GENERALIZED BELIAEV-POPOV THEORY

A consistent theory which goes beyond the mean-field approximation and takes into account collisions between

out-of-condensate quasi-particles was developed by Beliaev for a dilute Bose gas at  $T = 0$ .<sup>7</sup> A generalization of this for finite temperature was done by Popov.<sup>8</sup> The Beliaev-Popov approximation is the next step beyond the lowest order gapless theory and provides a consistent second-order self-energy approximation for the weakly interacting dilute Bose gas. It gives a gapless excitation spectrum with the velocity equal to the macroscopic speed of the sound at  $T = 0$ , in agreement with the findings by Gavoret and Nozières<sup>9</sup> which is valid to all orders in a perturbation theory treatment. For details on the underlying physics of the BPA we refer the reader to the review by Shi and Griffin.<sup>10</sup>

#### A. Effective interaction and higher-order contributions the self-energy

In this section the BPA is generalized to the case where the quasi-particles, interacting via a standard two-body potential, are moreover coupled by a phonon mediated retarded interaction. To construct the second-order self-energy diagrams we define an effective interaction as the sum of a two-body  $t$ -matrix and a phonon mediated retarded interaction  $\alpha^2\omega_0^2\mathcal{D}_0(\omega)$ , with  $\mathcal{D}_0(\omega)$  being given by the bare phonon Green's function.

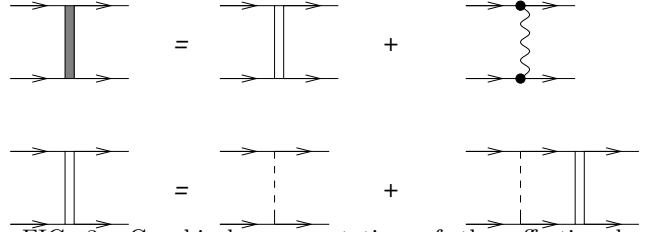


FIG. 3. Graphical representation of the effective boson-boson interaction.

The effective interaction is illustrated in Fig. 3 as a hatched line. The dashed line stands for the bare interaction potential and the non-hatched interaction line denotes the two-body  $t$ -matrix.

In Fig. 4 we reproduce all the Beliaev-Popov diagrams for the normal ( $\Sigma$ ) and anomalous ( $\hat{\Sigma}$ ) components of self-energy.<sup>10</sup> Each interaction line (hatched line) can be either a  $t$ -matrix or a phonon propagator. The diagrams are grouped in a way which is different from the conventional one. As it turns out this type of grouping is more convenient when it comes to summing up in a compact form the subset of self-energy diagrams involving the phonon mediated interaction. We use the standard notation of Green's function lines having cuts which indicate diagrams which are already included in the  $t$ -matrix and should be not counted again. The mean field approximation, discussed in the previous section, retains only the first two diagrams from the group  $a1$  and the first

diagram from the group  $a2$  in the normal and anomalous components of the self-energy respectively. The  $t$ -matrix is then being approximated by the  $s$ -wave scattering length.

Each second-order self-energy diagram consists of three contributions. The first contribution arises when both effective interaction lines are replaced by the  $t$ -matrix.

They have been extensively discussed in Ref. 10. The only difference between that and the case we want to study here is the four pole structure of the mean field Green's functions [see Eq. (20)]. The second contribution involves both the  $t$ -matrix and the phonon mediated interaction. Finally, the third contribution is exclusively due to the phonon mediated interaction.

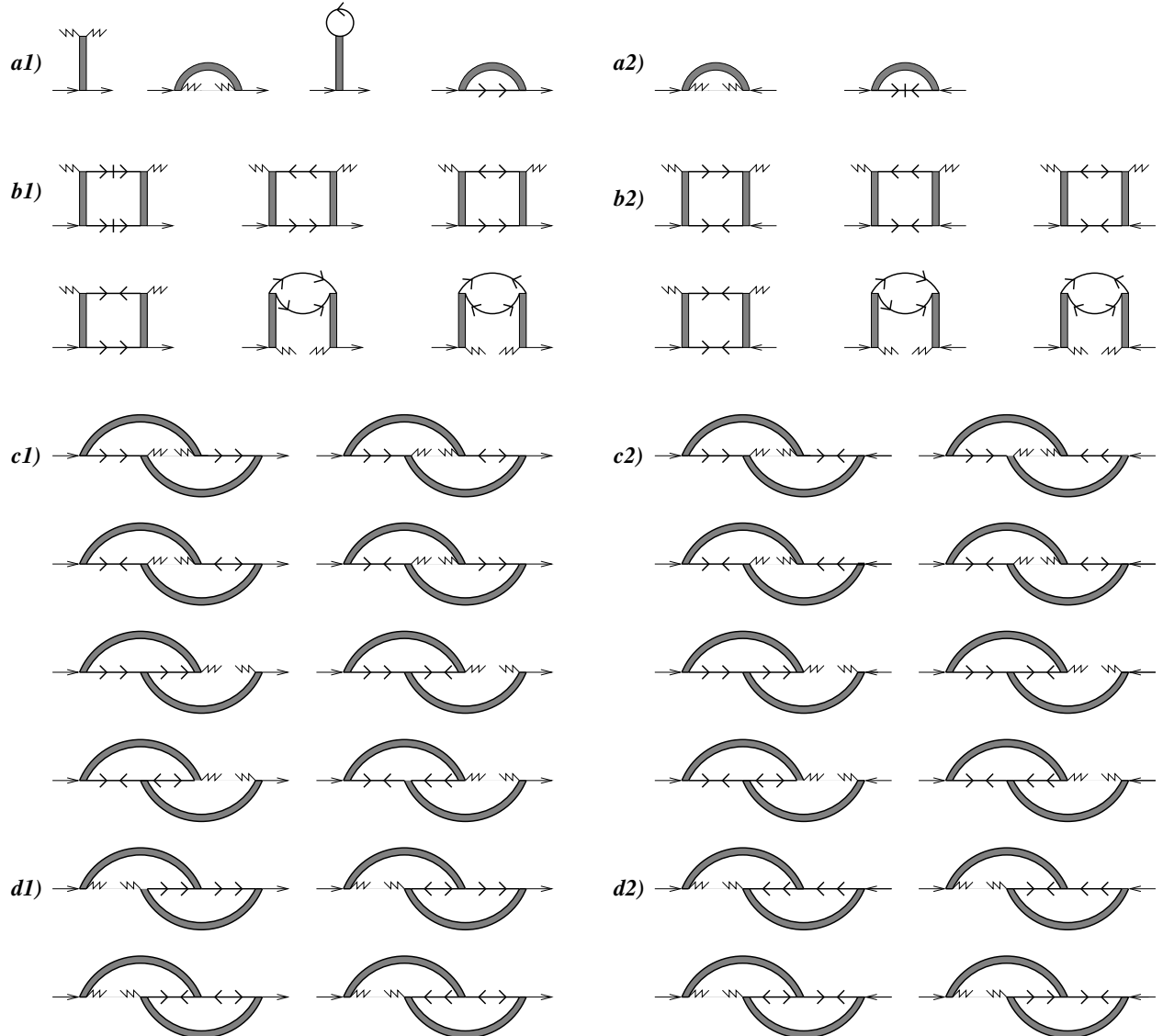


FIG. 4. Graphical representation, up to second-order in the effective interaction of all contributions to the normal and anomalous self-energy. The hatched lines represents the effective interaction shown in Fig. 3.

To sum up in the more compact form the subset of diagrams involving the boson-phonon coupling we use the graphical representation for the mean-field Green's functions, derived in the previous section [see Fig. 2]. We focus our discussion on the third subset of diagrams defined above. The second subset of diagrams, involving both types of interactions, are summed up using the same procedure. It turns out that the summation of the first

four diagrams from group  $b1$  together with the fourth diagram from group  $a1$  [see Fig. 4] is equivalent to replacing the bare phonon propagator in the last diagram by the mean-field propagator. As a result one arrives at the first diagram shown in Fig. 5. Similarly, the summation of the first four diagrams from the group  $c1$  in Fig. 4 leads to the second diagram in Fig. 5. The latter one represents the convolution of the Green's functions

describing the boson-phonon hybridization. The other diagrams in Fig. 5 and the ones for the anomalous self-energy, represented in Fig. 6, are obtained in the similar way.

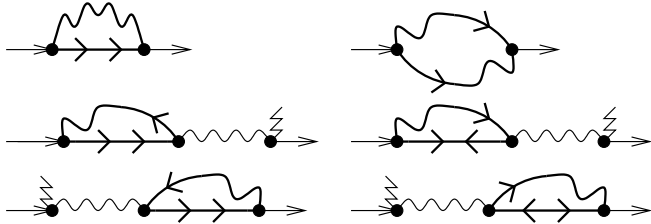


FIG. 5. Graphical representation, up to second-order in the phonon mediated boson-boson interaction, of the normal self-energy  $\Sigma$  due to the phonon mediated interaction.

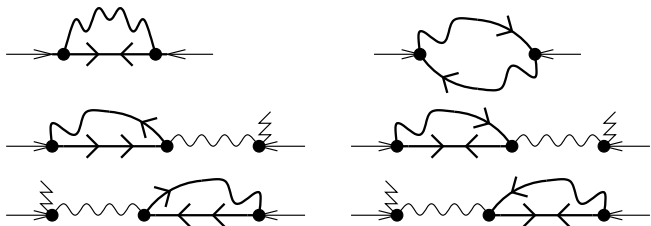


FIG. 6. Graphical representation up to second-order in the phonon mediated boson-boson interaction, of the anomalous self-energy  $\hat{\Sigma}$  due to the phonon-mediated interaction.

We would like to point out that, in the present treatment, the renormalization of the phonon mode as well as of all relevant vertex corrections is consistently taken into account up to the second-order in the effective interaction. The phonon mode is indeed renormalized by the density fluctuation of bosons. In the condensed state the density response function consists of two contributions: a quasi-particle part and a part describing density fluctuation of out-of-condensate particles. The phonon renormalization due to the first contribution is already present in the extended Bogoliubov scheme, leading to the renormalized (mean-field) propagator of phonons. By replacing the effective interaction by phonon propagators, one verifies that the first diagram from group a1 in Fig. 4 together with last two diagrams from group b1 describe the phonon mode renormalization arising from the density fluctuations of out-of-condensate particles. They are described given by the ‘‘particle-hole’’ bubble diagrams built up from normal and anomalous mean-field (Bogoliubov) Green’s functions of the bosons. One farther verifies, that the diagrams from group d1 together with diagrams of identical topology from group c1 from Fig. 4 generates the vertex corrections to the boson-phonon as well as to the boson-boson vertex. For example, when all the effective interaction lines in these diagrams are replaced by the phonon mediated interaction, one obtains the vertex corrections to the phonon-boson interaction. Similarly appear the corrections to the boson-phonon vertex due to the boson-boson inter-

action (these diagrams are generated by replacing one effective interaction line by the boson-boson interaction line). When all the phonon lines in the above mentioned class of diagrams are replaced by boson-boson interaction lines one obtains the renormalization of the boson-boson interaction. In a similarly way we can generate the diagrams renormalizing the boson-boson interaction by the phonon-boson interaction.

The normal and anomalous components of the Boson Green’s functions are expressed in terms of the self-energy via the Dyson-Beliaev equation

$$\mathcal{G}_{\mathbf{q},\omega} = \frac{\omega + \epsilon_{\mathbf{q}} + \Sigma_{\mathbf{q},-\omega}}{D_{\mathbf{q},\omega}}, \quad \hat{\mathcal{G}}_{\mathbf{q},\omega} = \frac{-\hat{\Sigma}_{\mathbf{q},\omega}}{D_{\mathbf{q},\omega}}, \quad (21)$$

where  $\epsilon_{\mathbf{q}}$  is the bare excitation spectrum measured from the chemical potential  $\mu$ . In Eq. (21) the following notations are introduced:

$$\begin{aligned} D_{\mathbf{q},\omega} &= [\omega - \mathcal{A}_{\mathbf{q},\omega}]^2 - [\epsilon_{\mathbf{q}} + S_{\mathbf{q},\omega}][\epsilon_{\mathbf{q}} + S_{\mathbf{q},\omega} + 2\hat{\Sigma}_{\mathbf{q},\omega}], \\ \mathcal{A}_{\mathbf{q},\omega} &= \frac{\Sigma_{\mathbf{q},\omega} - \Sigma_{\mathbf{q},-\omega}}{2}, \\ S_{\mathbf{q},\omega} &= \frac{\Sigma_{\mathbf{q},\omega} + \Sigma_{\mathbf{q},-\omega} - 2\hat{\Sigma}_{\mathbf{q},\omega}}{2}. \end{aligned} \quad (22)$$

Here  $\mathcal{A}_{\mathbf{q},\omega}$  is an antisymmetric function in  $\omega$ , while  $S_{\mathbf{q},\omega}$  and  $\hat{\Sigma}_{\mathbf{q},\omega}$  are symmetric functions of  $\omega$ . Invoking the Hugenholtz-Pines theorem (see the following sub-section) we have the relation  $\mu = \Sigma_{0,0} - \hat{\Sigma}_{0,0} = S_{0,0}$ .

The existence of the two branches in the excitation spectrum, Eq. (11) leads to three different contributions to the self-energy, describing the intra-band and inter-band scattering processes. Based on the mean-field Green’s functions, Eq. (20), we evaluate the above introduced dynamical quantities at zero temperature and arrive at the following result:

$$\begin{aligned} \mathcal{A}_{\mathbf{q},\omega} &= \frac{1}{N} \sum_{\mathbf{k},\alpha,\beta} \frac{A_{\alpha,\beta}(\mathbf{k},\mathbf{q})\omega}{\omega^2 - (\omega_{\alpha,\mathbf{k}} + \omega_{\beta,\mathbf{k}+\mathbf{q}})^2}, \\ S_{\mathbf{q},\omega} &= \frac{1}{N} \sum_{\mathbf{k},\alpha,\beta} \frac{S_{\alpha,\beta}(\mathbf{k},\mathbf{q})(\omega_{\alpha,\mathbf{k}} + \omega_{\beta,\mathbf{k}+\mathbf{q}})}{\omega^2 - (\omega_{\alpha,\mathbf{k}} + \omega_{\beta,\mathbf{k}+\mathbf{q}})^2}, \\ \hat{\Sigma}_{\mathbf{q},\omega} &= \frac{1}{N} \sum_{\mathbf{k},\alpha,\beta} \frac{M_{\alpha,\beta}(\mathbf{k},\mathbf{q})(\omega_{\alpha,\mathbf{k}} + \omega_{\beta,\mathbf{k}+\mathbf{q}})}{\omega^2 - (\omega_{\alpha,\mathbf{k}} + \omega_{\beta,\mathbf{k}+\mathbf{q}})^2}. \end{aligned} \quad (23)$$

$\alpha$  ( $\beta$ ) denotes the branch index,  $\beta \leq \alpha = 1, 2$ , the corresponding vertices  $A_{\alpha,\beta}$ ,  $S_{\alpha,\beta}$ , and  $M_{\alpha,\beta}$  which are expressed in terms of the coupling constants and coherence factors and are given in Appendix A.

The renormalized quasi-particle spectrum is given by the poles of the dressed boson Green’s function, or equivalently by the zeros of  $D_{\mathbf{q},\omega}$ . In the next section we discuss the long-wave length excitation spectrum of the system, focusing on the effect of boson-phonon coupling on the sound-velocity renormalization.

## B. The Hugenholtz-Pines theorem

One of the fundamental results in the theory of Bose systems is the Hugenholtz-Pines theorem<sup>11</sup> which relates the chemical potential to the self-energy in the condensed state via the relation

$$\mu = \Sigma_{0,0} - \hat{\Sigma}_{0,0}. \quad (24)$$

This theorem implies that the excitation spectrum of the system is gapless. However in certain approximations, for example the Hartree-Fock-Bogoliubov approximation (HFB), higher-order terms in the chemical potential are retained, while being neglecting in the self-energies. Such approximations are not "consistent" to any given order in the coupling constants and can generate an unphysical gap in the excitation spectrum of the system. Let us now verify this point for our treatment. We first calculate the chemical potential from the Heisenberg equations of motion for the Bose field (analogous to the Gross-Pitaevskii equation) and compare the result to that obtained from the Hugenholtz-Pines theorem. Our further treatment closely follows that of Ref. 12.

We start from the exact Heisenberg equation of motion for the Bose field  $b_{\mathbf{q}}$

$$i\dot{b}_{\mathbf{q}} = [\varepsilon_{\mathbf{q}} - \mu]b_{\mathbf{q}} + \frac{g}{N} \sum_{\mathbf{k}, \mathbf{p}} b_{\mathbf{k}+\mathbf{p}}^\dagger b_{\mathbf{k}+\mathbf{q}} b_{\mathbf{p}} - \frac{\alpha\omega_0}{\sqrt{N}} \sum_{\mathbf{k}, \mathbf{q}} b_{\mathbf{k}+\mathbf{q}} [a_{\mathbf{k}}^\dagger + a_{-\mathbf{k}}]. \quad (25)$$

The next step is to separate out the condensate part as in Eq. (2) and treat the boson interaction term in a self-consistent mean-field approximation (HFB approximation).<sup>12</sup> As a result we arrive at the following equation

$$\mu\bar{b} = gn_c\bar{b} + \frac{g}{N} \sum_{\mathbf{q}} \left[ 2\langle \hat{b}_{\mathbf{q}}^\dagger \hat{b}_{\mathbf{q}} \rangle + \langle \hat{b}_{\mathbf{q}}^\dagger \hat{b}_{\mathbf{q}} \rangle \right] \bar{b} - 2\alpha^2\omega_0 n\bar{b} - \frac{\alpha\omega_0}{\sqrt{N}} \sum_{\mathbf{q}} \langle \hat{b}_{\mathbf{q}} [\hat{a}_{\mathbf{q}}^\dagger + \hat{a}_{-\mathbf{q}}] \rangle, \quad (26)$$

where  $\bar{b}^2/N = n_c$  is the condensate fraction and  $n$  is the boson density. The above equation yields the following result for the chemical potential:

$$\mu = \mu_1 + \mu_2, \quad \mu_1 = \bar{g}n, \quad \mu_2 = g[\tilde{n} + \tilde{m}] - \alpha\omega_0\tilde{h}, \quad (27)$$

$\tilde{n}$ ,  $\tilde{m}$  denote the density and anomalous density of out-of-condensate particles, respectively and  $\tilde{h}$  is the strength of boson-phonon hybridization. These quantities are given by

$$\tilde{n} = \frac{1}{N} \sum_{\mathbf{q}} \langle \hat{b}_{\mathbf{q}}^\dagger \hat{b}_{\mathbf{q}} \rangle, \quad \tilde{m} = \frac{1}{N} \sum_{\mathbf{q}} \langle \hat{b}_{\mathbf{q}} \hat{b}_{\mathbf{q}} \rangle, \\ \tilde{h} = \frac{1}{\sqrt{n_c N}} \sum_{\mathbf{q}} \langle \hat{b}_{\mathbf{q}} [\hat{a}_{\mathbf{q}}^\dagger + \hat{a}_{-\mathbf{q}}] \rangle. \quad (28)$$

So far we did not make any approximation for the boson-phonon interaction. We next show that if all the above defined averages are calculated self-consistently from the corresponding mean field Green's functions, then the derived chemical potential Eq. (27) will coincide with that obtained from the Hugenholtz-Pines theorem.

In Fig. 7 we represent graphically the contributions to the chemical potential, Eq. (27), arising from the coupling of the bosons with the phonons. Putting this contribution together with the first contribution to  $\mu_2$  in Eq. (27) we obtain  $\mu_2 = A + \hat{A}$ .  $A$  and  $\hat{A}$  are the contributions corresponding to the fourth diagram from the group  $a1$  and the second diagram from the group  $a2$ , presented in Fig. 4.

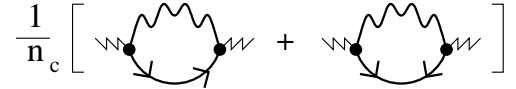


FIG. 7. Graphical representation of second-order contributions to the chemical potential due to the coupling with phonons.

Now we calculate the chemical potential from the Hugenholtz-Pines theorem. Examining the various diagrams of  $\Sigma_{0,0}$  and  $\hat{\Sigma}_{0,0}$  we find that most of them cancel pairwise, giving the following result

$$\mu_{\text{HP}} = \bar{g}n + g[\tilde{n} + \tilde{m}_{\text{R}}] + A - \hat{A} + B, \\ \tilde{m}_{\text{R}} = \tilde{m} - \frac{gn_c}{N} \sum_{\mathbf{q}} \frac{1}{2\varepsilon_{\mathbf{q}}}. \quad (29)$$

$\tilde{m}_{\text{R}}$  denotes the "renormalized" anomalous density<sup>12</sup> and

$$B = \frac{1}{N} \sum_{\mathbf{q}} \int d\omega n_c [g - \alpha^2\omega_0^2 \mathcal{D}_0(\omega)]^2 \{ \mathcal{G}_\omega \mathcal{G}_{-\omega} - [\hat{\mathcal{G}}_\omega]^2 \}.$$

Using the Dyson-Beliaev equation (21) we verify the following identities

$$2\hat{\mathcal{G}}_\omega = n_c [g - \alpha^2\omega_0^2 \mathcal{D}_0(\omega)] \{ \mathcal{G}_\omega \mathcal{G}_{-\omega} - [\hat{\mathcal{G}}_\omega]^2 \}, \\ B = \frac{2}{N} \sum_{\mathbf{q}} \int d\omega [g - \alpha^2\omega_0^2 \mathcal{D}_0(\omega)] \hat{\mathcal{G}}_\omega = 2\hat{A}. \quad (30)$$

Substituting the expressions, Eq. (30) into Eq. (29) we see that the chemical potential derived from the Hugenholtz-Pines theorem coincides with the one obtained from the Heisenberg equations of motion, Eq. (27).

## IV. RESULTS AND DISCUSSION

In the preceding section we have given the expressions for the self-energies in the Beliaev-Popov approximation. We now use these results to calculate the second-order corrections to the sound velocity and the chemical potential.

### A. Depletion of the ground state

We first discuss, the depletion of the ground state. From the Green's function Eq. (20) we determine the density of out-of-condensate particles  $\tilde{n}$ , and thus obtain the self-consistent equation for the density of particles in the condensate:

$$n = n_c + \tilde{n}, \quad \tilde{n} = \frac{1}{N} \sum_{\mathbf{k}} [v_{1,\mathbf{k}}^2 + \tilde{v}_{1,\mathbf{k}}^2] \quad (31)$$

$$= \frac{1}{N} \sum_{\mathbf{k}} \left\{ \frac{[\tilde{g}n_c + \varepsilon_{\mathbf{k}}][\omega_0 + \bar{E}_{\mathbf{k}}]}{2\bar{E}_{\mathbf{k}}(\omega_{1,\mathbf{k}} + \omega_{2,\mathbf{k}})} + \frac{\alpha^2 \omega_0 n_c}{\omega_{1,\mathbf{k}} + \omega_{2,\mathbf{k}}} - \frac{1}{2} \right\},$$

$\bar{E}_{\mathbf{q}} = \sqrt{\varepsilon_{\mathbf{q}}[\varepsilon_{\mathbf{q}} + 2\tilde{g}n_c]}$  is the spectrum of Bogoliubov quasi-particles with reduced scattering length  $\tilde{g}$  [see Eq. (3)]. The self-consistent equation for the condensate fraction, Eq. (31), is solved numerically. In Fig. 8 the relative depletion  $r = \tilde{n}/n$  as a function of density is presented for various values of the boson-phonon coupling constant  $\alpha$ . As clearly evident from this figure, for vanishing  $\alpha$ , the relative depletion follows the canonical  $\sqrt{n}$  behavior, which is characteristic for the dilute weakly interacting Bose gas. For a non-zero coupling constant however,  $r$  remains finite in the limit  $n \rightarrow 0$ , indicating a linear in density contribution to the depletion of the ground state.

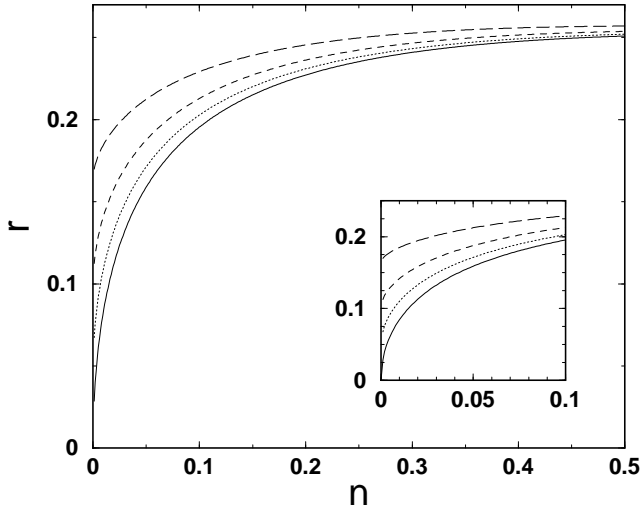


FIG. 8. Relative depletion of the ground state  $r = \tilde{n}/n$  as a function of density for different values of coupling constants ( $\alpha = 0, 1, 1.5$ , and  $2$  – solid line, dotted, dashed and long dashed lines, respectively) for  $\omega_0 = 0.2$  and  $g=3$ .

For  $n \ll 1$ , expanding the denominator in the last sum of Eq. (31) and keeping the leading order contributions in  $n_c$  we arrive at the following expression

$$\tilde{n} \simeq \frac{1}{N} \sum_{\mathbf{k}} \left[ \frac{\tilde{g}n_c + \varepsilon_{\mathbf{k}} - \bar{E}_{\mathbf{k}}}{2\bar{E}_{\mathbf{k}}} + \frac{\alpha^2 \omega_0^2 n_c}{(\omega_0 + \bar{E}_{\mathbf{k}})^2} \right]. \quad (32)$$

The first term in Eq. (32) gives rise to the canonical  $n_c^{3/2}$

contribution to the ground state depletion while the second term leads to the linear in density contribution, and is due to the boson-phonon coupling.

### B. The chemical potential

The second order contribution to the chemical potential is given as a sum of two contributions:  $\mu_2 = \mu_b + \mu_p$ . The first one is due to the boson-boson interaction and the second one stems from the boson-phonon interaction:

$$\mu_b = g(\tilde{n} + \tilde{m}_R) = \frac{g}{2N} \sum_{\mathbf{k}} \left[ \frac{\varepsilon_{\mathbf{k}}}{\bar{E}_{\mathbf{k}}} \frac{\omega_0 + \bar{E}_{\mathbf{k}}}{\omega_{1,\mathbf{k}} + \omega_{2,\mathbf{k}}} + \frac{gn_c}{\varepsilon_{\mathbf{k}}} - 1 \right],$$

$$\mu_p = -\alpha\omega_0\tilde{h} = -\alpha^2\omega_0^2 \sum_{\mathbf{k}} \frac{\varepsilon_{\mathbf{k}}}{\bar{E}_{\mathbf{k}}(\omega_{1,\mathbf{k}} + \omega_{2,\mathbf{k}})}. \quad (33)$$

In the normal state, where  $n_c = 0$ , the second contribution  $\mu_p$  coincides with the density independent negative shift of the chemical potential due to the coupling with phonons. However, in the condensed state this contribution becomes density dependent, via the density dependence of the spectrum in the condensed state. The density dependent part of this contribution increases with increasing density and hence gives rise to an increase of the system's compressibility. In Fig. 9 we plot the density dependent part of this contribution ( $\mu_p = \mu_p(n) - \mu_0(0)$ ) for several coupling constants.

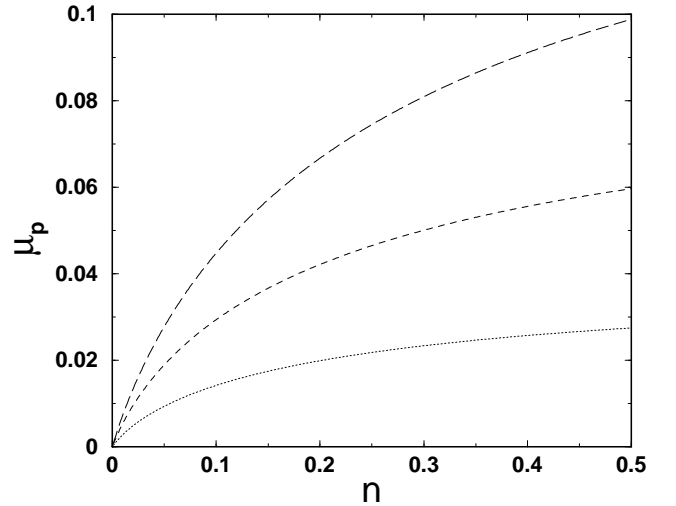


FIG. 9. Second order contribution to the chemical potential due to the boson-phonon coupling ( $\mu_p$ ) versus density ( $n$ ). ( $\alpha = 1, 1.5$ , and  $2$  – dotted, dashed and long dashed lines, respectively;  $\omega_0 = 0.2$  and  $g=3$ ).

The total second order correction to the chemical potential is presented in Fig. 10 which also shows its increase with  $\alpha$ . We would like to emphasize that for  $\alpha = 0$  and for  $n \rightarrow 0$  the second order correction to the chemical potential shows the canonical  $n^{3/2}$  behavior, while for



large  $\alpha$  the slope of  $\mu_2$  is almost linear [see inset on Fig. 10].

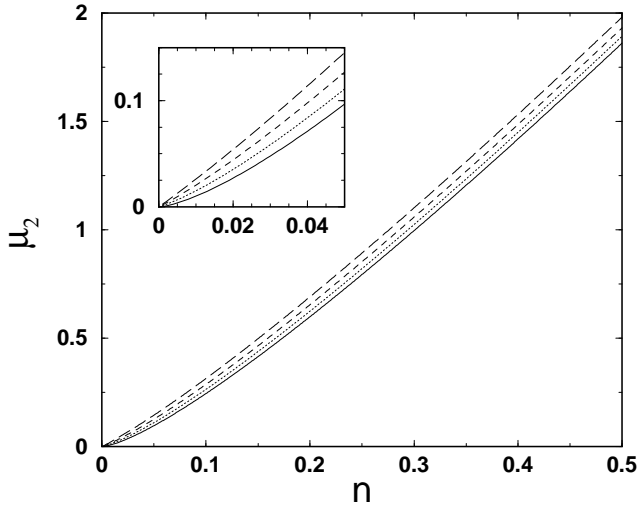


FIG. 10. Second order contribution to the chemical potential  $\mu_2$  vs density. ( $\alpha = 0, 1, 1.5,$  and  $2$  – solid, dotted, dashed and long dashed lines, respectively,  $\omega_0 = 0.2$  and  $g = 3$ ).

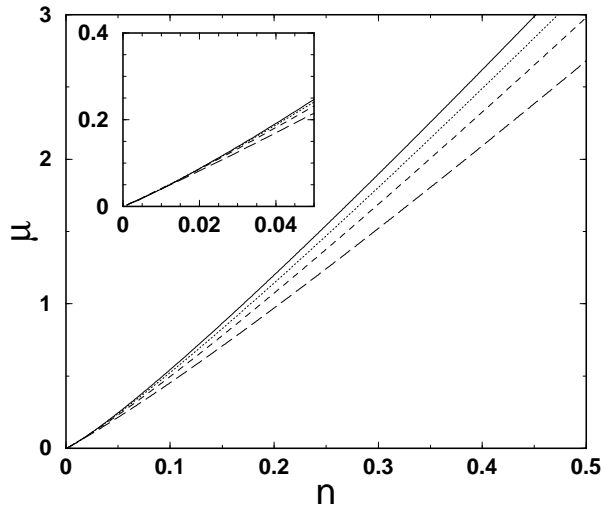


FIG. 11. Chemical potential  $\mu$  vs density  $n$ . ( $\alpha = 0, 1, 1.5,$  and  $2$  – solid, dotted, dashed and long dashed lines, respectively,  $\omega_0 = 0.2$  and  $g = 3$ ).

Keeping only terms in leading order in the density, the expression for  $\mu_b$  Eq. (33) becomes

$$\mu_b \simeq \frac{g}{N} \sum_{\mathbf{k}} \left\{ \left[ \frac{\bar{g}n_c + \varepsilon_{\mathbf{k}} - \bar{E}_{\mathbf{k}}}{2\bar{E}_{\mathbf{k}}} + \frac{gn_c}{2} \left( \frac{1}{\varepsilon_{\mathbf{k}}} - \frac{1}{\bar{E}_{\mathbf{k}}} \right) \right] + \alpha^2 \omega_0^2 n_c \frac{\omega_0 + 2\bar{E}_{\mathbf{k}}}{\bar{E}_{\mathbf{k}}(\omega_0 + \varepsilon_{\mathbf{k}})^2} \right\}. \quad (34)$$

It is the contribution in square brackets in Eq. (34), which leads to the canonical  $n^{3/2}$  behavior of the chemical potential. On the contrary, the second term, which is due

to boson-phonon coupling, is linear in density. Upon increasing  $\alpha$  this latter contribution to the chemical potential increases while the term proportional to  $n^{3/2}$  decreases, because of the reduction of the effective scattering length  $\bar{g}$ . This behavior is clearly seen from Fig. 11, where the chemical potential  $\mu = \mu_1 + \mu_2$  is illustrated as a function of density. For small  $n$  the contribution linear in density is dominating and the reduction of the chemical potential due to the phonon-mediated effective attraction in lowest order is almost canceled by the second order contribution. As a result, the slope of  $\mu$  is almost independent of  $\alpha$  at small densities [see the inset in Fig. 11], while at higher values of  $n$  the chemical potential decreases with increasing of  $\alpha$ , because of a decrease of the contribution proportional to  $n^{3/2}$ .

### C. The renormalized sound velocity

The renormalized quasi-particle spectrum, arising from the second order self-energy corrections, are given by the poles of the Boson Green's function (21), or equivalently by the zeros of  $D_{\mathbf{q},\omega}$  (23). Expanding the self-energies in the long-wavelength and low frequency limit around the mean field spectrum, we obtain the renormalized sound velocity  $v$  as

$$v = v_0[1 + \lambda]. \quad (35)$$

$v_0 = \sqrt{\bar{g}n_c/M}$  denotes the mean field sound velocity and  $\lambda$  the velocity renormalization factor given by

$$\lambda = \hat{\Sigma}_{0,0}^{(2)} / (2\bar{g}n_c) + \bar{g}n_c s - a. \quad (36)$$

$\hat{\Sigma}_{0,0}^{(2)}$  denotes the second order correction to the anomalous self-energy. The symmetric and antisymmetric self-energies, to leading order in  $\omega$  and  $\mathbf{q}$  [see Eq. (23)], are given by

$$s = \lim_{\mathbf{q} \rightarrow 0} \frac{\mathcal{S}_{\mathbf{q},\omega_{1,\mathbf{q}}} - \mu}{\omega_{1,\mathbf{q}}^2}, \quad a = \lim_{\mathbf{q} \rightarrow 0} \frac{\mathcal{A}_{\mathbf{q},\omega_{1,\mathbf{q}}}}{\omega_{1,\mathbf{q}}}. \quad (37)$$

Each of the three contributions entering in sound velocity renormalization factor, Eq. (36), contains infrared divergences, which are inherent to the Bose condensed state. However, as in the case of the standard weakly interacting Bose gas, these divergent terms are exactly canceled out in the final result for the low-frequency excitation spectrum. We have checked this cancellation analytically, picking up the divergent terms both due to the coherence factors and the existence of the gapless mode.

In Fig. 12 the sound velocity renormalization factor is presented for various values of the coupling constant  $\alpha$ . In the absence of boson-phonon coupling  $\lambda$  follows the canonical square root behavior in the density.<sup>10</sup> An increase of  $\alpha$  results in an overall enhancement of  $\lambda$  and moreover leads to a finite value of  $\lambda$ , even for vanishing density. As a result, the renormalized sound velocity

[see Fig. 13] is almost unaffected by the coupling of the bosons with phonons, in contrast to its mean field result, which is also presented in Fig. 13.

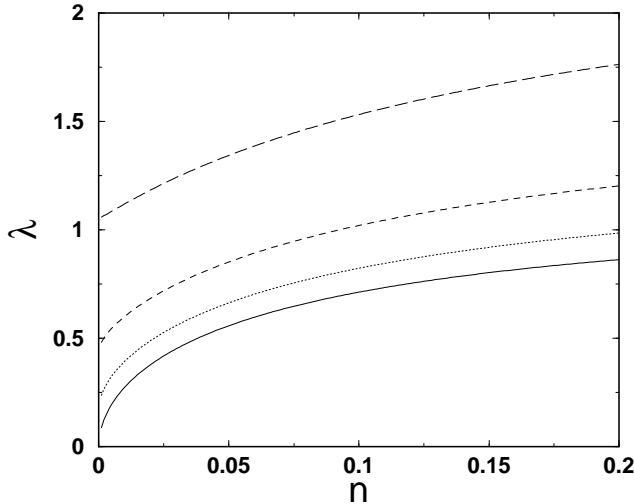


FIG. 12. Velocity renormalization factor  $\lambda$  versus density  $n$ . ( $\alpha=0, 1, 1.5$ , and  $2$  – solid, dotted, dashed and long dashed lines, respectively,  $\omega_0 = 0.2$  and  $g = 3$ ).

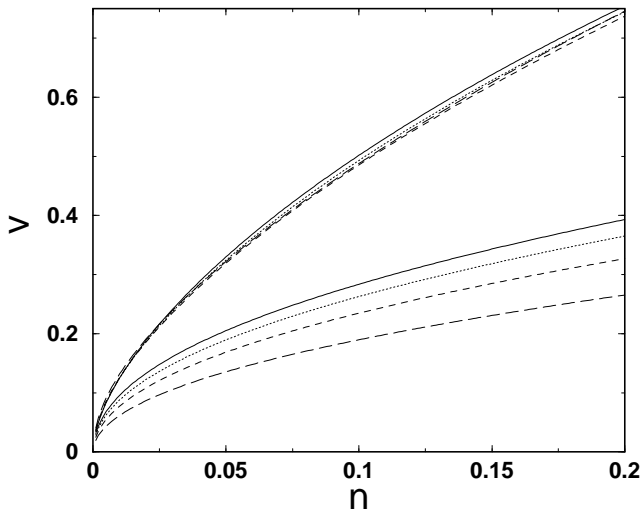


FIG. 13. Renormalized sound velocity  $v$  (upper curves), mean-field sound velocity (lower curves) versus the density  $n$  ( $\alpha=0, 1, 1.5$ , and  $2$  – solid, dotted, dashed and long dashed lines, respectively.  $\omega_0 = 0.2$  and  $g = 3$ ).

The interesting question now is, why the boson dressing effects, leading to its mass enhancement, does not show up in the velocity renormalization factor. Responsible for the mass enhancement is the first diagram in Fig. 5 for the normal self-energy. It is frequency dependent and is finite in the limit  $n \rightarrow 0$ . It gives a positive contribution to  $a$  and hence a negative contribution to the sound velocity [see Eq. (36)]. It turns out that in the condensed state there are two effects that overcom-

pensate this negative contribution. First, the effective boson-phonon coupling is no longer local and becomes momentum dependent because of the coherence factors. It is decreased in the condensed state. For the momentum transfer equal to the wavevector at which the level crossing of the bare modes occurs, this effective interaction is exactly zero. The second main important contribution competing with this diagram is contained in the first diagram illustrated in Fig. 6 for the anomalous self-energy. This diagram is positive, thus leading to a positive contribution to the anomalous part of inter-particle potential, and hence increases the sound velocity.

In Fig. 14 we present these two contribution for various  $\alpha$ , rescaling them by a factor  $(\alpha^2 \omega_0^2)^{-1}$ . As can be seen from this figure there is almost an exact cancellation of these two contributions for different  $\alpha$ . That explains the absence of the density independent negative contribution to the sound velocity originating from the boson mass enhancement.

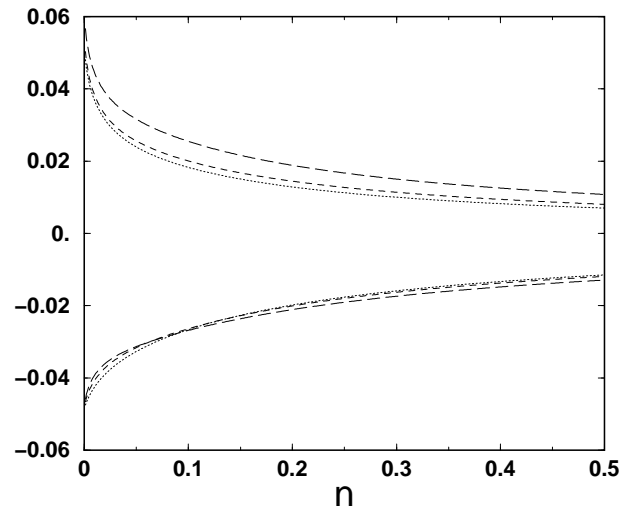


FIG. 14. The negative (positive) contribution to the sound velocity renormalization factor from normal (anomalous) second order diagrams illustrated by the first diagram in Fig.5 (Fig. 6) ( $\alpha = 1, 1.5$ , and  $2$  – dotted, dashed and long dashed lines, respectively,  $\omega_0 = 0.2$  and  $g = 3$ ).

## V. CONCLUSION

In the present paper we have considered the problem of a system of bosons on a deformable lattice which, apart from an intrinsic repulsion between them, are coupled to local lattice deformations - treated in terms of Einstein phonon modes. This leads to a retarded time dependent contribution to the effective two-body vertex. When the bosons condense, the phonons, being initially coupled to the boson density (symmetry restoring variable in the case of gauge symmetry breaking), get hybridized with the Goldstone mode. The generalized Bogoliubov transformation has been used to diagonalize the bilinear part of Hamiltonian describing the excitation spectra of the

system in the lowest order approximation. As a result two dispersion branches have been obtained: one describing a gapless sound-wave like mode and one exhibiting a gap. The two normal modes describe Bogoliubov type excitations and Einstein phonons. For momenta close to where the level crossing of bare excitation spectra occurs neither mode is predominantly a phonon or a Bogoliubov quasi-particle.

The ground state depletion is shown to consist of two contributions: the first one showing the canonical  $n^{3/2}$  behavior in the density and the second one, which appears because of the retarded phonon mediated interaction, being linear in density. The relative depletion of the ground state remains finite in the limit  $n \rightarrow 0$  because of retardation effects.

The sound velocity obtained in this approximation is reduced due to reduction of the repulsive boson-boson interaction, arising from the attractive part of phonon mediated interaction in the static limit.

Considering the second order corrections to the chemical potential and excitation spectrum, the Beliaev-Popov theory has been generalized to our case. For that purpose an effective interaction has been introduced and all second-order self-energy diagrams were constructed in terms of this interaction. The short range bare boson-boson two-body potential has been renormalized in the standard way by summing up the ladder diagrams and introducing the two-body  $t$ -matrix with the characteristic  $s$ -wave scattering length. Since the phonon mediated boson-boson interaction, vanishes at high frequencies as  $1/\omega^2$ , this interaction does not require any special renormalization in order to avoid ultraviolet divergences in the case of continuum model. Due to the pole structure of phonon mediated interaction, the density of bosons no longer enters in the expansion parameter and one has to assume a small value of boson-phonon coupling constant in order to treat the problem by perturbation theory.

Unlike the lowest order results, the second order contribution to both the chemical potential and the sound velocity shows an increase with the boson-phonon coupling constant and contains a term linear in the density which is exclusively due to the retarded nature of phonon mediated interaction. As a result the total chemical potential and the sound velocity obtained within this theory are practically unaffected by the coupling to the phonons. This effect is more pronounced in the low density limit  $n \ll 1$ . One might ascribe this effect to the robustness of the superfluid state.

In the present paper we have restricted ourself to the case when the boson system is coupled to optical phonon

modes of the lattice. The formalism developed here can be easily extended to the case of acoustic phonons. In such a scenario the two normal modes correspond to two types of sound modes: the acoustic phonon mode of the lattice and the Goldstone mode of condensed Bose system. The effect of the coupling between these two sound modes as well as as well as damping effects can be treated within the present formalism. However, in that case the coupling with  $q = 0$  phonon mode (representing translation of the whole crystal) should be discarded. It amounts to neglecting the Hartree type contribution to the boson self-energy due to the phonon mediated interaction.

The present study induces us to speculate on the possibility of an insulator to superconducting transition when the boson-phonon coupling constant is strong. In that case the mass renormalization of the bosons varies exponentially with the coupling constant as  $\exp(\alpha^2)$  when we consider the normal state of the system. In the superfluid state we expect again a phase stiffness of the condensate practically unaffected by the coupling of the bosons to the lattice vibrations. Possibly such features exist in the cuprate superconductors which show a resistivity which, upon lowering the temperature, tends to an insulating behavior before abruptly dropping to zero when the system becomes superconducting. Similarly, upon entering the superconducting state, out of the broad incoherent contribution to the angle resolved photo-emission spectra evolves a sharp resonance peak which could suggest well defined quasi-particles in the superconducting state and totally diffusive modes in the normal state. Within the physics developed in the present study we can speculate on an undressing of the bosons as the temperature is lowered and the transition from the normal into the superfluid state takes place. These and related questions will be addressed in some future work.

## ACKNOWLEDGMENTS

One of the authors (G. J) acknowledges support from a *bourse de Recherche Scientifique et technique de l'OTAN* and from an INTAS Program, Grant No 97-0963 and No 97-11066. He acknowledges in particular the kind hospitality at the Centre de Recherches sur les Très Basses Températures, where the main part of the present work has been carried out and the Max-Planck Institute für Physik komplexer Systeme, where the final part of the work has been completed.

## APPENDIX: EFFECTIVE VERTICES

As we have already mentioned in the main text, each self-energy contribution introduced in Eq. (23) consist of three different parts describing the intra-band (denoted as 11(22) for the scattering within the lower (upper) branch) and inter-band (denoted as 12) scattering processes. The vertices for inter-band scattering are given by

$$\begin{aligned}
A_{12}(\mathbf{k}, \mathbf{q}) &= 4g^2 n_c \left[ (u_{1,\mathbf{k}}^2 \bar{u}_{1,\mathbf{k}+\mathbf{q}}^2 - v_{1,\mathbf{k}}^2 \bar{v}_{1,\mathbf{k}+\mathbf{q}}^2) - 2u_{1,\mathbf{k}} v_{1,\mathbf{k}} (\bar{u}_{1,\mathbf{k}+\mathbf{q}}^2 - \bar{v}_{1,\mathbf{k}+\mathbf{q}}^2) - 2\bar{u}_{1,\mathbf{k}+\mathbf{q}} \bar{v}_{1,\mathbf{k}+\mathbf{q}} (u_{1,\mathbf{k}}^2 - v_{1,\mathbf{k}}^2) \right] \\
&\quad - 4g\alpha\omega_0\sqrt{n_c} \left[ (u_{2,\mathbf{k}} - v_{2,\mathbf{k}}) \{ (u_{1,\mathbf{k}} - v_{1,\mathbf{k}}) (\bar{u}_{1,\mathbf{k}+\mathbf{q}}^2 - \bar{v}_{1,\mathbf{k}+\mathbf{q}}^2) - (u_{1,\mathbf{k}} + v_{1,\mathbf{k}}) \bar{u}_{1,\mathbf{k}+\mathbf{q}} \bar{v}_{1,\mathbf{k}+\mathbf{q}} \} \right. \\
&\quad \left. + (\bar{u}_{2,\mathbf{k}+\mathbf{q}} - \bar{v}_{2,\mathbf{k}+\mathbf{q}}) \{ (\bar{u}_{1,\mathbf{k}+\mathbf{q}} - \bar{v}_{1,\mathbf{k}+\mathbf{q}}) (u_{1,\mathbf{k}}^2 - v_{1,\mathbf{k}}^2) - (\bar{u}_{1,\mathbf{k}+\mathbf{q}} + \bar{v}_{1,\mathbf{k}+\mathbf{q}}) u_{1,\mathbf{k}} v_{1,\mathbf{k}} \} \right] \\
&\quad + 8g\alpha^2\omega_0 n_c \left[ u_{1,\mathbf{k}} v_{1,\mathbf{k}} (\bar{u}_{1,\mathbf{k}+\mathbf{q}}^2 - \bar{v}_{1,\mathbf{k}+\mathbf{q}}^2) + \bar{u}_{1,\mathbf{k}+\mathbf{q}} \bar{v}_{1,\mathbf{k}+\mathbf{q}} (u_{1,\mathbf{k}}^2 - v_{1,\mathbf{k}}^2) \right] \\
&\quad - 2\alpha^3\omega_0^2\sqrt{n_c} \left[ \{ (u_{2,\mathbf{k}} - v_{2,\mathbf{k}}) (\bar{u}_{1,\mathbf{k}+\mathbf{q}} + \bar{v}_{1,\mathbf{k}+\mathbf{q}}) + (\bar{u}_{2,\mathbf{k}+\mathbf{q}} - \bar{v}_{2,\mathbf{k}+\mathbf{q}}) (u_{1,\mathbf{k}} + v_{1,\mathbf{k}}) \} \{ u_{1,\mathbf{k}} \bar{v}_{1,\mathbf{k}+\mathbf{q}} + \bar{u}_{1,\mathbf{k}+\mathbf{q}} v_{1,\mathbf{k}} \} \right] \\
&\quad + \alpha^2\omega_0^2 \left[ (u_{2,\mathbf{k}} - v_{2,\mathbf{k}})^2 (\bar{u}_{1,\mathbf{k}+\mathbf{q}}^2 - \bar{v}_{1,\mathbf{k}+\mathbf{q}}^2) + (\bar{u}_{2,\mathbf{k}+\mathbf{q}} - \bar{v}_{2,\mathbf{k}+\mathbf{q}})^2 (u_{1,\mathbf{k}}^2 - v_{1,\mathbf{k}}^2) \right. \\
&\quad \left. + 2(u_{2,\mathbf{k}} - v_{2,\mathbf{k}}) (\bar{u}_{2,\mathbf{k}+\mathbf{q}} - \bar{v}_{2,\mathbf{k}+\mathbf{q}}) (u_{1,\mathbf{k}} \bar{u}_{1,\mathbf{k}+\mathbf{q}} - v_{1,\mathbf{k}} \bar{v}_{1,\mathbf{k}+\mathbf{q}}) \right] \\
S_{12}(\mathbf{k}, \mathbf{q}) &= 4g^2 n_c \left[ u_{1,\mathbf{k}} \bar{u}_{1,\mathbf{k}+\mathbf{q}} - v_{1,\mathbf{k}} \bar{v}_{1,\mathbf{k}+\mathbf{q}} \right]^2 \\
&\quad - 4g\alpha\omega_0\sqrt{n_c} \left[ (u_{1,\mathbf{k}} \bar{u}_{1,\mathbf{k}+\mathbf{q}} - v_{1,\mathbf{k}} \bar{v}_{1,\mathbf{k}+\mathbf{q}}) \{ (u_{2,\mathbf{k}} - v_{2,\mathbf{k}}) (\bar{u}_{1,\mathbf{k}+\mathbf{q}} + \bar{v}_{1,\mathbf{k}+\mathbf{q}}) + (\bar{u}_{2,\mathbf{k}+\mathbf{q}} - \bar{v}_{2,\mathbf{k}+\mathbf{q}}) (u_{1,\mathbf{k}} + v_{1,\mathbf{k}}) \} \right] \\
&\quad + \alpha^2\omega_0^2 \left[ (u_{2,\mathbf{k}} - v_{2,\mathbf{k}})^2 (\bar{u}_{1,\mathbf{k}+\mathbf{q}} + \bar{v}_{1,\mathbf{k}+\mathbf{q}})^2 + (\bar{u}_{2,\mathbf{k}+\mathbf{q}} - \bar{v}_{2,\mathbf{k}+\mathbf{q}})^2 (u_{1,\mathbf{k}} + v_{1,\mathbf{k}})^2 \right] \\
M_{12}(\mathbf{k}, \mathbf{q}) &= 8g^2 n_c \left[ (u_{1,\mathbf{k}}^2 \bar{v}_{1,\mathbf{k}+\mathbf{q}}^2 + \bar{u}_{1,\mathbf{k}+\mathbf{q}}^2 v_{1,\mathbf{k}}^2) - u_{1,\mathbf{k}} v_{1,\mathbf{k}} (\bar{u}_{1,\mathbf{k}+\mathbf{q}}^2 + \bar{v}_{1,\mathbf{k}+\mathbf{q}}^2) \right] \\
&\quad - 2\bar{u}_{1,\mathbf{k}+\mathbf{q}} \bar{v}_{1,\mathbf{k}+\mathbf{q}} (u_{1,\mathbf{k}}^2 + v_{1,\mathbf{k}}^2) + 3u_{1,\mathbf{k}} v_{1,\mathbf{k}} \bar{u}_{1,\mathbf{k}+\mathbf{q}} \bar{v}_{1,\mathbf{k}+\mathbf{q}} \\
&\quad + 4g\alpha\omega_0\sqrt{n_c} \left[ 2\{ (u_{1,\mathbf{k}} - v_{1,\mathbf{k}}) (u_{2,\mathbf{k}} - v_{2,\mathbf{k}}) \bar{u}_{1,\mathbf{k}+\mathbf{q}} \bar{v}_{1,\mathbf{k}+\mathbf{q}} + (\bar{u}_{1,\mathbf{k}+\mathbf{q}} - \bar{v}_{1,\mathbf{k}+\mathbf{q}}) (\bar{u}_{2,\mathbf{k}+\mathbf{q}} - \bar{v}_{2,\mathbf{k}+\mathbf{q}}) u_{1,\mathbf{k}} v_{1,\mathbf{k}} \} \right. \\
&\quad \left. + \{ (u_{2,\mathbf{k}} - v_{2,\mathbf{k}}) (\bar{u}_{1,\mathbf{k}+\mathbf{q}} - \bar{v}_{1,\mathbf{k}+\mathbf{q}}) + (\bar{u}_{2,\mathbf{k}+\mathbf{q}} - \bar{v}_{2,\mathbf{k}+\mathbf{q}}) (u_{1,\mathbf{k}} - v_{1,\mathbf{k}}) \} (u_{1,\mathbf{k}} \bar{v}_{1,\mathbf{k}+\mathbf{q}} + \bar{u}_{1,\mathbf{k}+\mathbf{q}} v_{1,\mathbf{k}}) \right] \\
&\quad - 8g\alpha^2\omega_0 n_c \left[ 2(u_{1,\mathbf{k}} \bar{v}_{1,\mathbf{k}+\mathbf{q}} + \bar{u}_{1,\mathbf{k}+\mathbf{q}} v_{1,\mathbf{k}})^2 - u_{1,\mathbf{k}} v_{1,\mathbf{k}} (\bar{u}_{1,\mathbf{k}+\mathbf{q}}^2 + \bar{v}_{1,\mathbf{k}+\mathbf{q}}^2) - \bar{u}_{1,\mathbf{k}+\mathbf{q}} \bar{v}_{1,\mathbf{k}+\mathbf{q}} (u_{1,\mathbf{k}}^2 + v_{1,\mathbf{k}}^2) \right] \\
&\quad - 2\alpha^3\omega_0^2\sqrt{n_c} \left[ (u_{1,\mathbf{k}} - v_{1,\mathbf{k}}) (u_{2,\mathbf{k}} - v_{2,\mathbf{k}}) \bar{u}_{1,\mathbf{k}+\mathbf{q}} \bar{v}_{1,\mathbf{k}+\mathbf{q}} + (\bar{u}_{1,\mathbf{k}+\mathbf{q}} - \bar{v}_{1,\mathbf{k}+\mathbf{q}}) (\bar{u}_{2,\mathbf{k}+\mathbf{q}} - \bar{v}_{2,\mathbf{k}+\mathbf{q}}) u_{1,\mathbf{k}} v_{1,\mathbf{k}} \right. \\
&\quad \left. + (u_{2,\mathbf{k}} - v_{2,\mathbf{k}}) (\bar{u}_{1,\mathbf{k}+\mathbf{q}}^2 v_{1,\mathbf{k}} - \bar{v}_{1,\mathbf{k}+\mathbf{q}}^2 u_{1,\mathbf{k}}) + (\bar{u}_{2,\mathbf{k}+\mathbf{q}} - \bar{v}_{2,\mathbf{k}+\mathbf{q}}) (u_{1,\mathbf{k}}^2 \bar{v}_{1,\mathbf{k}+\mathbf{q}} - v_{1,\mathbf{k}}^2 \bar{u}_{1,\mathbf{k}+\mathbf{q}}) \right] \\
&\quad + 8\alpha^4\omega_0^2 n_c \left[ u_{1,\mathbf{k}} \bar{v}_{1,\mathbf{k}+\mathbf{q}} + \bar{u}_{1,\mathbf{k}+\mathbf{q}} v_{1,\mathbf{k}} \right]^2 \\
&\quad - 2\alpha^2\omega_0^2 \left[ (u_{2,\mathbf{k}} - v_{2,\mathbf{k}})^2 \bar{u}_{1,\mathbf{k}+\mathbf{q}} \bar{v}_{1,\mathbf{k}+\mathbf{q}} + (\bar{u}_{2,\mathbf{k}+\mathbf{q}} - \bar{v}_{2,\mathbf{k}+\mathbf{q}})^2 u_{1,\mathbf{k}} v_{1,\mathbf{k}} \right. \\
&\quad \left. + (u_{2,\mathbf{k}} - v_{2,\mathbf{k}}) (\bar{u}_{2,\mathbf{k}+\mathbf{q}} - \bar{v}_{2,\mathbf{k}+\mathbf{q}}) (u_{1,\mathbf{k}} \bar{v}_{1,\mathbf{k}+\mathbf{q}} + v_{1,\mathbf{k}} \bar{u}_{1,\mathbf{k}+\mathbf{q}}) \right]. \tag{A1}
\end{aligned}$$

The corresponding vertices for the transitions within the lower (upper) band are obtained from the above expressions by replacing  $\bar{u}, \bar{v} \rightarrow u, v$  ( $u, v \rightarrow \bar{u}, \bar{v}$ ) and multiplying by a factor  $1/2$ .

<sup>†</sup> On leave of absence from Institute of Physics, Georgian Academy of Sciences, 380077 Tbilisi, Georgia.

<sup>1</sup> A. Griffin, *Excitations in a Bose-Condensed Liquid* (Cambridge University Press, 1993).

<sup>2</sup> A. Mysyrowicz, E. Benson, and E. Fortin, Phys. Rev. Lett. **77**, 896 (1996); T. Goto, M. Y. Shen, S. Koyama, and T. Yokuchi, Phys. Rev. B **55**, 7609 (1997).

<sup>3</sup> I. Loutsenko and D. Roubtsov, Phys. Rev. Lett. **78**, 3011 (1997).

<sup>4</sup> R.P. Sharma, T. Venkatesan, Z.H. Zhang, J. R. Liu, R. Chu

and W. K. Chu, Phys. Rev. Lett. **77**, 4624 (1996).

<sup>5</sup> G. Ruani and P. Ricci, Phys. Rev. B **55**, 93 (1997); O. V. Misochko, E. Ya. Sherman, N. Umesaki and S. Nakashima, Phys. Rev. B **59**, 11495 (1999).

<sup>6</sup> N. N. Bogoliubov, J. Phys. USSR **5**, 23 (1947).

<sup>7</sup> S. T. Beliaev, Sovjet Physics JETP **7**, 299 (1958).

<sup>8</sup> V.N. Popov, "Functional Integrals in Quantum Field theory and Statistical Physics", Ch. 6, Reidle, Dortrecht (1983)

<sup>9</sup> J. Gavoret and P. Nozières, Ann. Phys. (New York) **28**, 349 (1964).

<sup>10</sup> H. Shi and A. Griffin, Phys. Rep. **304**, 1 (1998).

<sup>11</sup> N. M. Hugenholtz and D. Pines, Phys. Rev. **116**, 489 (1959).

<sup>12</sup> A. Griffin, Phys. Rev. B **53**, 9341 (1996).